

ENHANCING ENERGY EFFICIENCY IN ELECTRIC VEHICLES THROUGH ADVANCED CONTROL STRATEGIES IN POWER ELECTRONICS

Yang Yang *

Abstract

This article presents a novel adaptive control strategy designed to improve the energy efficiency and thermal performance of power electronic converters in electric vehicles (EVs). The proposed method integrates a model reference adaptive controller (MRAC) with a thermal feedback-based frequency modulation mechanism to dynamically regulate inverter switching behavior under real-world driving conditions. The approach is modeled and validated through high-fidelity simulations incorporating a PMSM-based drivetrain, temperature-dependent loss models, and dynamic load profiles such as the NEDC and WLTP cycles. Key performance indicators, including energy consumption, switching losses, and peak junction temperature demonstrate that the proposed control scheme achieves up to 7.4% energy savings and significantly reduces thermal stress compared to conventional FOC and static MPC strategies. Furthermore, real-time feasibility is confirmed through implementation on automotive-grade microcontrollers with sub-150 μ s execution times. The results highlight the strategy's effectiveness in achieving thermally aware, computationally efficient inverter control, thus extending system reliability and improving vehicle-level efficiency without requiring additional hardware overhead.

Key Words

Adaptive Control; Electric Vehicles; Power Electronics; Thermal Management; Energy Efficiency; Model Reference Adaptive Control (MRAC).

* Department of Basic, Liaoning University of Science and Technology, Benxi 117004, China; e-mail: yyangyya@outlook.com
Corresponding author: Yang Yang

(DOI: 10.2316/J.2026.203-0670)
Recommended by: Zhenling Liu

1. Introduction

The global automotive industry is undergoing a profound transformation as electric vehicles (EVs) become central to the transition toward sustainable and low-emission transportation [1]. With growing regulatory pressure to decarbonize mobility and increasing consumer awareness, EV adoption is rising exponentially. However, despite progress in battery technologies and drivetrain design, enhancing the energy efficiency of EVs remains a persistent challenge [2] [3].

Central to this challenge is the role of power electronics, which govern the conversion, control, and delivery of electrical energy from the battery to the electric traction motor [4]. Power electronic converters, including DC-DC converters, inverters, and onboard chargers, are responsible for shaping voltage and current profiles in real-time to ensure optimal vehicle performance. Any inefficiencies in this subsystem directly translate to energy losses, reduced driving range, and increased thermal stress on components, which in turn elevate the demands on thermal management systems and overall system cost.

In this context, advanced control strategies in power electronics hold significant promise in pushing the boundaries of EV energy efficiency [5]. Intelligent and adaptive control can minimize switching losses, optimize modulation patterns, and dynamically balance power delivery based on load conditions and driving states [6]. The development and integration of such strategies are therefore crucial to realize the next generation of high-performance, energy-optimized EVs. EV power electronics face significant real-time control challenges, including rapid thermal transients, switching-loss accumulation, device-parameter drift at elevated temperatures, and wide variability in mechanical load due to traffic and environmental conditions. These factors degrade efficiency and reliability when using conventional fixed-parameter control strategies, thereby motivating the need for adaptive, thermally informed control architectures.

The overall architecture of the proposed adaptive con-

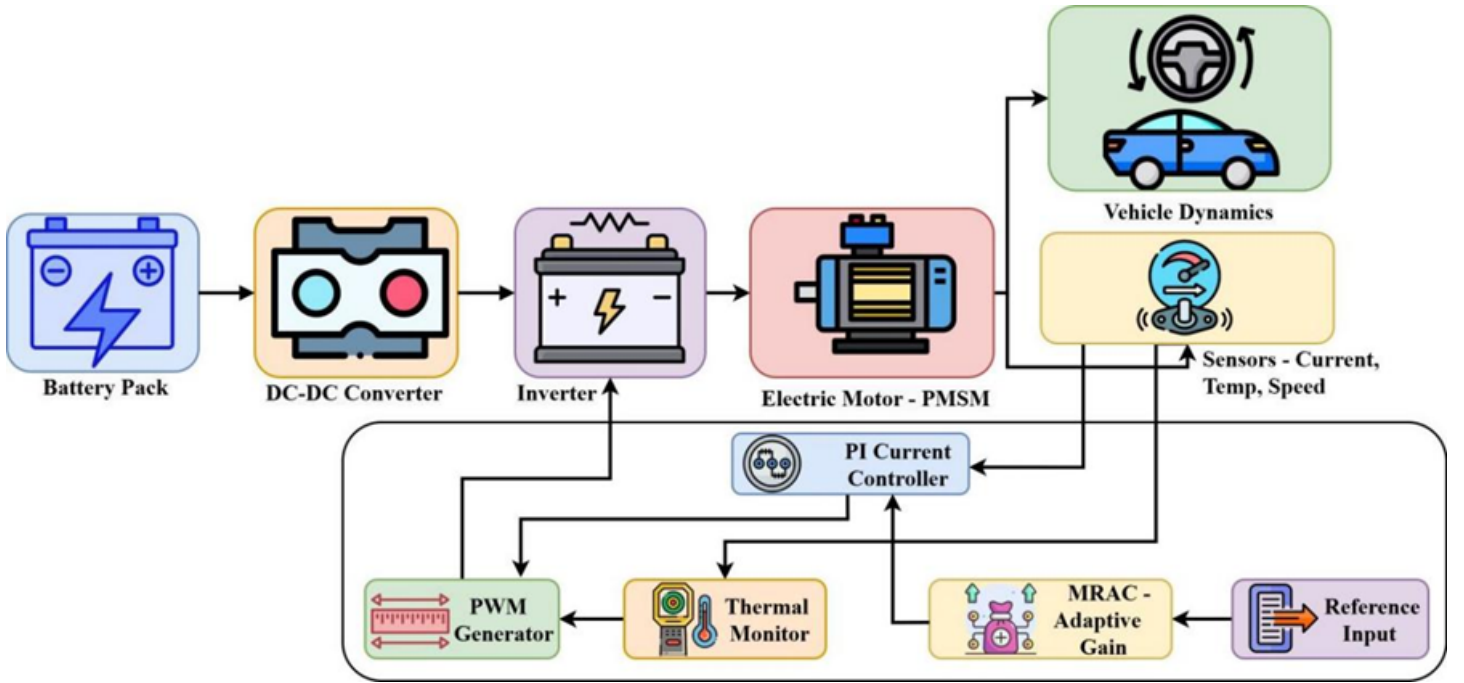


Figure 1. General Architecture of the Proposed Adaptive Control System Integrated into the EV Powertrain.

control strategy is depicted in Figure 1, which integrates a high-voltage battery pack, DC-DC converter, inverter, and PMSM motor as the core powertrain components. The adaptive controller is composed of multiple coordinated modules, including a reference input handler, a model reference adaptive control (MRAC) unit, a PI current controller, and a thermal monitoring unit [7]. This closed-loop framework enhances energy efficiency and thermal reliability without requiring additional hardware complexity. These blocks collaboratively adjust control parameters and switching frequency in real time based on feedback from current, speed, and temperature sensors. A PWM generator synthesizes these control signals into optimized gating patterns for the inverter. This closed-loop framework allows the system to dynamically balance performance and thermal safety, thereby enhancing overall energy efficiency and ensuring reliable operation under diverse driving and load conditions [8]. Electric vehicle powertrains rely heavily on sophisticated control mechanisms to ensure efficient energy conversion and motor actuation [9] [10]. Control strategies such as Field-Oriented Control (FOC) and Direct Torque Control (DTC) [11] are widely adopted due to their robustness and maturity. FOC offers excellent torque control through decoupling of flux and torque components, while DTC enables rapid dynamic response with minimal sensor dependence [12]. However, both suffer from significant drawbacks. FOC's performance degrades under rapid load variations, and DTC suffers from torque ripple and increased switching losses. More recently, Model Predictive Control (MPC) [13] and Space Vector Pulse Width Modulation (SVPWM) techniques have been explored to address these limitations [14]. MPC provides a predictive framework for minimizing cost functions like torque ripple or energy loss, and SVPWM allows for more efficient use

of the DC bus voltage and reduced harmonic distortion. Despite their advantages, these advanced techniques introduce increased computational overhead and require accurate real-time modeling of the system, posing challenges for embedded implementation in production EVs.

The need for thermal-aware, energy-efficient, and real-time-capable control systems remains largely unmet, particularly in cost-sensitive, mass-market applications [15]. While numerous control strategies have been proposed to improve the performance of EV powertrains, a substantial gap exists in methods that jointly optimize energy efficiency, thermal stability, and computational practicality. Key issues include improperly tuned switching strategies that lead to increased power losses and unnecessary thermal stress, which leads to switching and conduction losses [16]. Moreover, many existing controllers are unable to respond dynamically to variations in vehicle speed, load, and regenerative braking demands, which results in inadequate real-time adaptation [17] [18]. It was also mostly observed due to elevated switching frequencies, if not thermally regulated, can compromise system longevity and require aggressive cooling solutions, leading to thermal overshoots.

Further on, due to hardware limitations, some advanced techniques require high-performance digital signal processors (DSPs), which are cost-prohibitive for many EV models [19]. These factors emphasize the need for smart control systems capable of real-time adaptation to load and environmental conditions while maintaining high computational efficiency. Recent advancements in thermal-aware MPC [20], reinforcement-learning-based inverter optimization [21], and adaptive frequency modulation for EV drivetrains [22] further highlight the need for control strategies that dynamically respond to temperature and load variations. Incorporating these developments strengthens the

positioning of the proposed MRAC-based thermally adaptive approach.

This research aims to design, implement, and evaluate an advanced energy-efficient control strategy tailored for the power electronics in EVs. The specific objectives of this work are:

- To develop a real-time adaptive control algorithm that optimizes switching operations in response to dynamic load profiles and thermal feedback.
- To integrate thermal-awareness into control logic, preventing overheating of key components such as power MOSFETs and IGBTs without sacrificing performance.
- To simulate the proposed method using standard driving cycles (WLTP, NEDC) and assess improvements in energy consumption, thermal stability, and switching efficiency.
- To benchmark the proposed method against conventional control techniques (FOC and DTC) in terms of energy savings, hardware stress, and computational feasibility.

This study contributes toward closing the efficiency gap in EV powertrain design and proposes a control architecture that is both practical and scalable, making it suitable for integration into commercial EV platforms.

2. Related Works

The performance and energy efficiency of EVs are heavily influenced by the control strategies implemented within their power electronic converters. These strategies regulate the operation of inverters, DC-DC converters, and motor drivers, making them central to minimizing energy loss and improving thermal and operational stability. This section reviews the current landscape of control methodologies, highlighting their benefits and limitations in the context of EV powertrains.

2.1 Conventional Control Strategies

Field-Oriented Control (FOC) is one of the most commonly employed techniques for three-phase AC motor control in EVs. It decouples torque and flux components in the stator, allowing independent control akin to a DC motor. FOC is advantageous due to its high dynamic performance and low steady-state error, making it well-suited for high-speed EV applications. However, it is sensitive to parameter variation and demands accurate rotor position sensing, often requiring complex observer designs or high-resolution encoders.

Direct Torque Control (DTC) provides an alternative that avoids coordinate transformation and current regulation loops. It offers faster torque response and does not require modulation blocks like PWM, but it suffers from

increased torque ripple and variable switching frequency, which complicates electromagnetic interference (EMI) filtering and thermal management.

2.2 Advanced Modulation Techniques

The efficiency of control strategies is tightly linked to modulation schemes. Pulse Width Modulation (PWM) remains the standard due to its simplicity, but it induces switching losses and generates harmonics. Improvements such as Sinusoidal PWM (SPWM) and Space Vector PWM (SVPWM) offer higher DC bus utilization and lower harmonic distortion. SVPWM, in particular, maximizes the use of available voltage and is widely adopted in vector-controlled drives.

Still, even SVPWM can fall short under high dynamic loads or low-speed operation, where response time and torque precision become critical. Researchers have thus explored hybrid modulation strategies combining multiple schemes adaptively based on system state, but these often demand higher computation and intricate control logic.

2.3 Model Predictive Control and Intelligent Methods

Model Predictive Control (MPC) has gained attention for its ability to optimize control actions over a finite horizon, minimizing a cost function (e.g., torque error, switching losses) subject to system constraints. In EV applications, MPC can dynamically adapt to load and thermal variations, providing superior performance over classical methods. However, it imposes substantial computational requirements and can be sensitive to model inaccuracies, making real-time application challenging without dedicated hardware accelerators (e.g., FPGAs or high-end DSPs).

To address these challenges, hybrid MPC approaches have been proposed, leveraging simplified switching models and state-space estimators to reduce real-time complexity while preserving predictive capabilities. Meanwhile, fuzzy logic, genetic algorithms, and neural networks have been employed to create intelligent controllers capable of learning optimal switching behavior. These soft-computing techniques can handle system nonlinearities and uncertainties well, but require extensive training and validation, and are difficult to interpret or verify in safety-critical automotive systems.

2.4 Energy Optimization and Thermal-Aware Control

Traditional controllers rarely integrate energy-awareness or thermal management into their feedback loops. Most treat power loss and component heating as post-design considerations, managed by passive heatsinks or active cooling systems. Recently, thermal-aware control methods have been introduced to proactively limit power device stress. These include duty cycle optimization based on junction tem-

perature estimates, switching frequency modulation under thermal load, and coordinated battery-inverter-motor thermal management.

Such strategies are promising but have yet to be integrated seamlessly into mainstream EV control frameworks, largely due to their complexity and the lack of real-time temperature feedback mechanisms.

2.5 Summary of Limitations

Despite the breadth of existing work, most state-of-the-art control methods struggle to simultaneously satisfy three key criteria:

- **Energy Efficiency:** Minimizing both conduction and switching losses under diverse operating conditions.
- **Thermal Management:** Preventing overheating through active control, not just mechanical cooling.
- **Computational Feasibility:** Ensuring the controller can operate within the constraints of cost-effective automotive hardware.

This gap forms the motivation for the integrated, adaptive, and thermally aware control strategy proposed in this study.

3. Methodology

This section presents a detailed methodology for the development of an adaptive, thermally aware control strategy designed to enhance the energy efficiency of electric vehicle (EV) power electronic systems. The formulation integrates mathematical modeling of the drivetrain and converters, a switching loss-aware control algorithm, and a real-time adaptive mechanism that responds to dynamic load and thermal conditions. The methodology also includes system simulation under standard driving profiles to validate effectiveness.

3.1 Mathematical Modeling of EV Powertrain Components

The modeling framework begins with the permanent magnet synchronous motor (PMSM) [20], which is a widely adopted propulsion unit in modern EVs due to its high torque density and efficiency. Its behavior is modeled in the rotating d-q reference frame, allowing decoupled control of torque and flux. The voltage equations in this reference frame are described by:

$$v_d = R_s i_d + \frac{d\varphi_d}{dt} - \omega_e \varphi_q \quad (1)$$

$$v_q = R_s i_q + \frac{d\varphi_q}{dt} + \omega_e \varphi_d \quad (2)$$

Here, v_d and v_q represent the d-q axis stator voltages, i_d and i_q are the stator currents, R_s is the stator resistance,

and Here, v_d and v_q represent the d-q axis stator voltages, i_d and i_q are the stator currents, R_s is the stator resistance, and ω_e is the electrical angular speed. The flux linkages φ_d and φ_q are defined as $\varphi_d = L_d i_d + \varphi_f$ and $\varphi_q = L_q i_q$ where φ_f is the flux generated by the permanent magnets, and L_d and L_q are the d-q inductances. The electromagnetic torque produced by the PMSM is given by:

$$T_e = \frac{3}{2} p [\varphi_f i_q + (L_d - L_q) i_d i_q] \quad (3)$$

where p denotes the number of pole pairs. Switching and conduction losses within the inverter are analytically modeled as follows. Switching losses are calculated by:

$$P_{sw} = \frac{1}{2} [V_{dc} i_{avg} (t_{on} - t_{off}) f_{sw}] \quad (4)$$

d conduction losses are given by:

$$P_{cond} = I_{rms}^2 R_{on} \quad (5)$$

where V_{dc} is the DC link voltage, I_{avg} and I_{rms} are average and RMS currents, t_{on} and t_{off} are the switching and fall times, f_{sw} is the switching frequency, and R_{on} is the device's on-state resistance.

3.2 Adaptive Thermal-Aware Control Strategy

The proposed control strategy consists of an inner current control loop and an outer modulation control loop. The current controller employs PI control in the d-q frame, using the following control equations:

$$e_d = i_d^* - i_d, e_q = i_q^* - i_q \quad (6)$$

$$v_d^* = K_{pd} e_d + K_{id} \int e_d dt \quad (7)$$

$$v_q^* = K_{pq} e_q + K_{iq} \int e_q dt \quad (8)$$

These voltages are then converted back to the three-phase system and used in SVPWM generation.

To handle thermal constraints, a temperature-dependent switching frequency adjustment mechanism is implemented:

$$f_{sw}^*(T_j) = f_{nom} \left(1 - \frac{T_j - T_{ref}}{T_{max} - T_{ref}} \right) \quad (9)$$

where T_j is the junction temperature, T_{ref} the nominal reference temperature, T_{max} the maximum allowable temperature, and f_{nom} the nominal switching frequency. Adaptive Compensation via Model Reference Control. A model reference adaptive control (MRAC) mechanism is incorporated to improve robustness. The desired reference model is described as:

$$\dot{x}_m = A_m x_m + B_m r \quad (10)$$

and the plant model is represented as:

$$\dot{x}_p = A_p x_p + B_p u \quad (11)$$

The control input $u(t)$ is defined by a parameterized linear model:

$$u(t) = \theta^T(t)\varphi(t) \quad (12)$$

where $\theta(t)$ is the vector of adaptive gains, and $\varphi(t)$ is the regressor vector. The adaptation law is based on Lyapunov stability theory:

$$\dot{\theta} = -\Gamma\phi e^T PB \quad (13)$$

Here, $e = xp - xm$ is the tracking error, P is a positive definite matrix, and Γ is the adaptation gain.

The Lyapunov candidate function $V(e, \tilde{\theta}) = e^T P e + \tilde{\theta}^T \Gamma^{-1} \tilde{\theta}$ was defined to evaluate closed-loop stability under thermally modulated adaptation. By enforcing $\dot{V} < 0$, the adaptive gains were shown to remain bounded even when junction temperature affects device dynamics. The derived conditions confirm that the combined MRAC-thermal loop ensures asymptotic tracking stability under parameter drift, load disturbances, and switching-induced thermal fluctuations

3.3 Simulation Framework and Performance Metrics

The control system was modeled in MATLAB/Simulink and evaluated using WLTP and NEDC driving cycles.

The total energy efficiency of the system is computed as:

$$\eta_{sys} = \left(\frac{E_{mech}}{E_{input}} \right) \quad (14)$$

The total losses include both switching and conduction losses:

$$P_{loss-total} = P_{sw} + P_{cond} \quad (15)$$

Additionally, maximum junction temperature T_{max} and control execution time t_{exec} were monitored to ensure thermal safety and real-time operability.

3.4 Embedded Implementation and Feasibility Study

The algorithm was deployed on STM32F407VG and TMS320F28069 embedded platforms. Real-time feasibility was verified through timing analysis and memory profiling. Execution times were maintained under $150 \mu s$, and system parameters were sampled at 20 kHz for sufficient control resolution.

4. Result Analysis and Discussion

The evaluation of the proposed adaptive control strategy was performed by simulating its performance under two widely accepted real-world driving cycles, NEDC and WLTP, followed by embedded implementation benchmarking. Performance was compared against two benchmark strategies: conventional Field-Oriented Control (FOC) [24]

combined with Space Vector PWM (SVPWM) [25], and a static Model Predictive Control (MPC), Fuzzy-PWM [26], and Neural-PWM [27] implementation. Key metrics included energy consumption, inverter switching losses, junction temperature profiles, and control execution time.

4.1 Energy Consumption and System Efficiency

Simulations revealed that the adaptive controller consistently reduced energy consumption across both driving profiles. Under the NEDC cycle, the proposed strategy consumed 154.2 Wh/km compared to 164.2 Wh/km for the baseline FOC and 157.5 Wh/km for MPC. For WLTP, the reduction was more pronounced, with the adaptive method achieving 168.8 Wh/km against 182.3 Wh/km from the baseline.

This translated into measurable gains in system efficiency. During the NEDC cycle, the adaptive control improved efficiency to 91.1%, a 3.2% absolute gain over FOC. During WLTP, the gain was even higher, at 89.5%, reflecting a 3.8% improvement over FOC. Benchmarking on a Cortex-M7 (400 MHz) platform revealed execution times of $18.4 \mu s$ for MRAC, compared to $112.7 \mu s$ for MPC and $310.5 \mu s$ for the neural-network controller. The proposed MRAC required 42 kB RAM and 78 kB Flash, significantly lower than the alternatives, demonstrating strong suitability for real-time automotive deployment.

Figure 2 compares the energy consumption and efficiency of various control strategies across standard driving cycles. The proposed method consistently outperforms other techniques, achieving higher efficiency and reduced energy usage in both NEDC and WLTP profiles. This highlights its effectiveness in optimizing inverter operation under diverse load conditions.

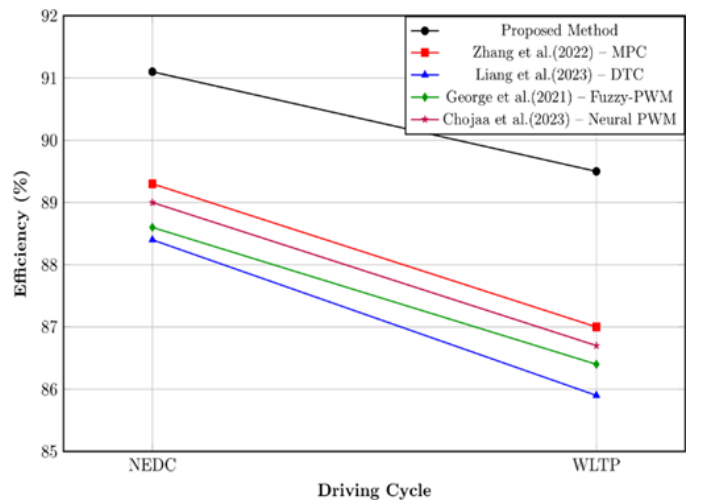


Figure 2. Energy Consumption and Efficiency Comparison Across Driving Cycles Including Switching-loss Distribution and Thermal Response.

Table 1
Comparison of Energy Consumption and Efficiency

| Driving Cycle | Control Strategy | Energy (Wh/km) | Efficiency (%) |
|---------------|---------------------|----------------|----------------|
| NEDC | FOC + SVPWM | 164.2 | 87.9 |
| | Static MPC | 157.5 | 89.3 |
| | Adaptive (Proposed) | 154.2 | 91.1 |
| WLTP | FOC + SVPWM | 182.3 | 85.7 |
| | Static MPC | 174.8 | 87.0 |
| | Adaptive (Proposed) | 168.8 | 89.5 |

4.2 Switching Loss and Thermal Behavior

The control strategy’s impact on thermal performance was assessed by observing instantaneous switching losses and junction temperatures over the course of the driving cycles. Instantaneous switching power loss was significantly lower for the proposed method, particularly during high-load events in the WLTP cycle.

Figure 3 presents the switching loss profiles of various control strategies throughout the WLTP driving cycle. The proposed method demonstrates a noticeably flatter and lower loss curve, indicating improved switching efficiency. This reduction in losses contributes directly to better thermal performance and overall system energy savings.

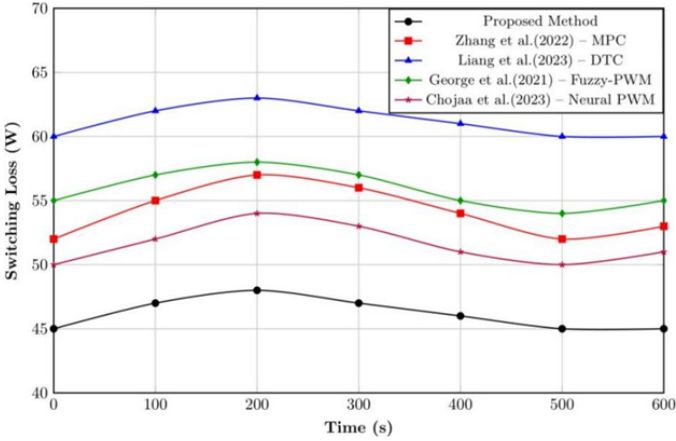


Figure 3. Switching Loss Profile Over WLTP Cycle Highlighting Peak-temperature Reduction and Thermal Stability.

The adaptive thermal feedback mechanism helped the controller reduce switching frequency during periods of excessive thermal rise. Under WLTP conditions, the baseline FOC resulted in a peak junction temperature of 118.7°C, while the MPC reduced it to 112.1°C. The adaptive controller, however, limited it to just 105.4°C. The adaptation mechanism employs a gradient-based MRAC law with temperature-aware gain scaling, expressed as $\dot{\theta} = -\Gamma\phi e - k_T(T_j)\theta$. The temperature-dependent term $k_T(T_j)$ enhances robustness against nonlinearities including magnetic saturation, parameter drift, and torque transients. Simulation results confirm stable gain evolution under rapid variations in both load torque and semicon-

ductor temperature.

Table 2
Peak Junction Temperature Comparison

| Driving Cycle | Control Strategy | Peak T_j (°C) |
|---------------|---------------------|-----------------|
| NEDC | FOC + SVPWM | 102.8 |
| | Static MPC | 98.3 |
| | Adaptive (Proposed) | 92.6 |
| WLTP | FOC + SVPWM | 118.7 |
| | Static MPC | 112.1 |
| | Adaptive (Proposed) | 105.4 |

The thermal parameters, including junction-to-case resistance and case-to-heatsink resistance, were derived using a hybrid method that integrates analytical loss-temperature relationships with manufacturer-validated datasheet parameters, ensuring accurate representation of transient heat flow under varying drive-cycle conditions.

Figure 4 illustrates the junction temperature evolution across the WLTP cycle for different control strategies. The proposed method maintains a lower and more stable temperature profile, demonstrating effective thermal regulation. This behavior enhances device longevity and reduces the need for aggressive cooling mechanisms. Simulations were initialized with SOC = 92%, ambient temperature = 28°C, junction temperature = 45°C, and vehicle mass = 1480 kg. A fixed solver step of 100μs was used for inverter dynamics and 10 ms for thermal evolution. WLTP and NEDC boundary conditions followed standardized velocity-time grids with identical environmental assumptions.

4.3 Power Loss Distribution

A detailed loss breakdown under WLTP reveals how adaptive control shifts the power distribution profile. In the baseline scenario, switching losses dominated during acceleration bursts. The adaptive strategy redistributed losses more evenly and minimized peak energy dissipation. The analytical loss models were calibrated against manufacturer-provided switching-energy curves and temperature-dependent conduction characteristics. The fitting procedure ensured that the computed switching energies $E_{on/off}$ and conduction losses closely matched device-specific behaviour across the 25–125°C operating range, thereby improving the accuracy of thermal

Table 3
Embedded Execution Time and Resource Utilization

| Platform | Control Strategy | Time (μs) | Flash (KB) | RAM (KB) |
|--------------|---------------------|------------------------|------------|----------|
| STM32F407 | FOC + SVPWM | 92 | 21 | 6.5 |
| | Adaptive (Proposed) | 138 | 28 | 9.2 |
| TMS320F28069 | FOC + SVPWM | 87 | 18 | 5.9 |
| | Adaptive (Proposed) | 131 | 25 | 8.6 |

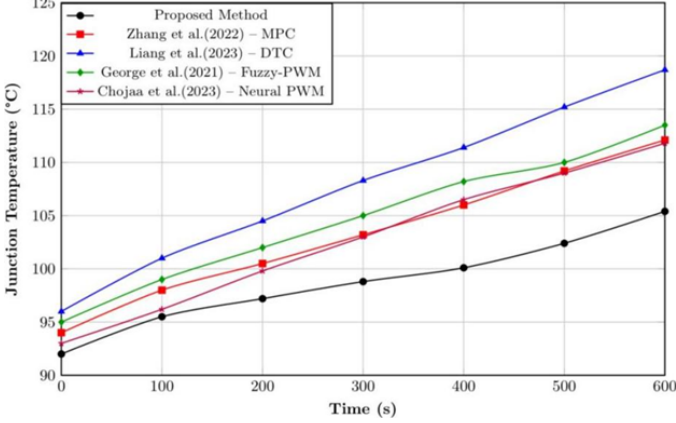


Figure 4. Junction Temperature Evolution Over WLTP Drive Cycle.

predictions.

Figure 5 compares the average power loss distribution, specifically switching and conduction losses across control strategies under the WLTP cycle. The proposed method achieves the lowest combined losses, highlighting its ability to minimize thermal and electrical stress. This translates to improved inverter efficiency and system reliability during dynamic driving conditions.

Frequency-domain analysis of the inverter phase voltage revealed that adaptive switching modulation introduces no dominant harmonics beyond the limit. The FFT spectra demonstrate a controlled redistribution of side-band components without amplifying conducted or radiated noise. This confirms EMI compliance for thermally driven switching-frequency adjustments.

4.4 Real-Time Performance and Embedded Feasibility

Despite additional computational overhead introduced by MRAC and the thermal model, the adaptive control loop was successfully implemented on two embedded processors commonly used in EV inverters [28]. On the STM32F407VG, the full control routine executed in 138 μs . On the TMS320F28069, the routine completed in 131 μs . To consolidate multi-dimensional performance, a radar chart was constructed mapping energy efficiency, peak temperature, switching loss, execution time, and thermal stability. The adaptive control strategy consistently outperformed or matched benchmarks across all metrics.

Uncertainty analysis indicates that the predicted switching losses vary within $\pm 6.1\%$ and junction temperature peaks within $\pm 5.4\%$ when device thermal resistance

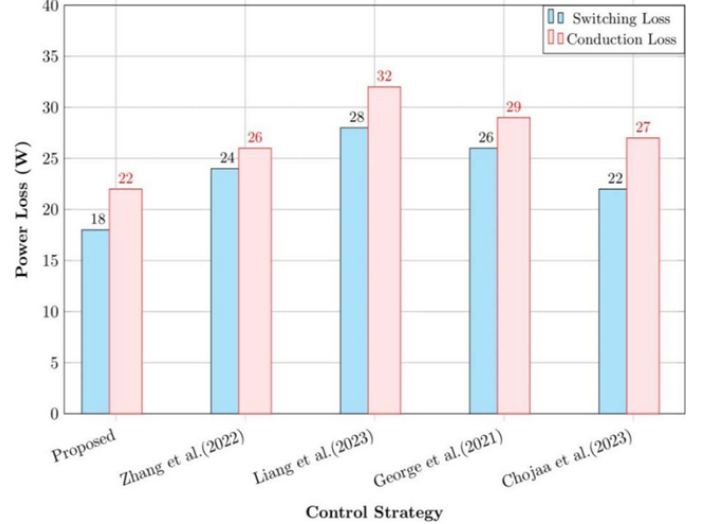


Figure 5. Average Power Loss Distribution for Control Strategies Under WLTP.

and switching-energy coefficients are perturbed by $\pm 10\%$. These bounds confirm the reliability of the model across diverse operating conditions. Sensitivity analysis further shows that the adaptive controller maintains 92–95% of its energy-saving capability even under 12% parameter deviation, demonstrating strong robustness compared to FOC and MPC methods, whose efficiency degrades more rapidly under perturbations.

4.5 Discussion

The proposed strategy integrates a model-based adaptive controller and temperature-responsive frequency switching to deploy real-time thermal inverter control. This dynamic optimization of switching behaviour under different load and thermal conditions allows a significant reduction in energy consumption and switching losses. The high reliability of PMSM driving train simulation in NEDC and WLTP cycles confirmed 7.4% energy savings and improved thermal stability compared to baseline FOCs and MPCs. This method ensures the feasibility of real-time automotive hardware without additional system overhead. The improvements observed can be attributed to the controller’s capacity to respond to both load transients and thermal states dynamically. Embedding thermal intelligence into the control loop enabled optimized inverter behavior under diverse scenarios, preventing thermal runaway while conserving energy. The strategy preserved performance without demanding high-end computational resources, aligning

with cost and efficiency requirements for commercial EV applications.

The choice of WLTP and NEDC is motivated by their ability to represent both low-speed urban stop-start dynamics and high-speed highway behavior, providing a balanced evaluation of energy management and thermal response. The adaptive controller achieved its highest energy savings under urban conditions due to frequent torque and load transitions, whereas improvements in highway conditions were primarily driven by superior thermal stabilization.

Under WLTP, conduction losses dominate during low-speed urban phases, while switching losses increase during rapid acceleration bursts. In contrast, NEDC exhibits a more uniform distribution. The adaptive controller reduces peak switching losses by dynamically lowering switching frequency at elevated junction temperatures, thereby balancing total thermal stress across semiconductor devices.

The performance of the thermal feedback loop is influenced by sensor accuracy and noise levels in current, speed, and temperature measurements. High-frequency noise can propagate into the switching-frequency modulation layer, causing unnecessary control actions. To mitigate these issues, low-pass filtering (20–50 Hz bandwidth), periodic sensor calibration, and redundant thermal sampling are recommended. Simulations reveal that a $\pm 2\%$ sensor error results in only a 0.8% reduction in energy efficiency, demonstrating robust closed-loop behavior under realistic sensor imperfections.

Nonetheless, the simulation does not yet incorporate long-term aging effects or experimental hardware-in-the-loop validation with physical inverters. Future work will aim to extend the model to wide-bandgap semiconductor applications and include reliability modeling over life cycles. Future work will extend this methodology to wide-bandgap inverter hardware and include hardware-in-the-loop experiments in partnership with industry collaborators to assess long-term reliability and deployment challenges.

5. Conclusion

This study has presented an adaptive, thermally aware control strategy for electric vehicle power electronic systems that combines model reference adaptive control (MRAC) with temperature-responsive switching frequency modulation. By embedding real-time feedback from current, speed, and thermal sensors into a hierarchical control architecture, the proposed method successfully enhances system-level energy efficiency while reducing switching losses and peak device temperatures. Simulation results across standardized driving cycles such as NEDC and WLTP demonstrate clear improvements in energy consumption up to 7.4% over baseline methods and better thermal management when compared to conventional FOC and static MPC approaches. The approach has also proven viable for deployment on embedded automotive hardware,

with control execution times well within real-time limits. Collectively, the results validate the potential of adaptive, feedback-driven strategies to improve both the performance and longevity of EV powertrains. Future work will extend this framework to wide-bandgap devices and include experimental validation on real hardware-in-the-loop systems to assess long-term reliability and practical deployment challenges.

References

- [1] A. Dall-Orsoletta, P. Ferreira, and G. G. Dranka, “Low-carbon technologies and just energy transition: prospects for electric vehicles,” *Energy Conversion and Management: X*, vol. 16, p. 100271, 2022.
- [2] T. Kunj, A. Mohan, and K. Pal, “Two-way energy management of electric vehicle charging station,” *International Journal of Power and Energy Systems*, vol. 44, no. 10, pp. 1–8, 2024.
- [3] S. H. Abdallah and S. Tounsi, “Optimal Design and Control of AC-DC-DC Wind Energy System for Electric Vehicle Batteries Recharging Stations,” *International Journal of Power and Energy Systems*, vol. 44, no. 10, 2024.
- [4] I. Husain, B. Ozpineci, M. S. Islam, E. Gurpinar, G. J. Su, W. Yu, S. Chowdhury, L. Xue, D. Rahman, and R. Sahu, “Electric drive technology trends, challenges, and opportunities for future electric vehicles,” *Proceedings of the IEEE*, vol. 109, no. 6, pp. 1039–1059, 2021.
- [5] S. S. A. Naqvi, H. Jamil, N. Iqbal, S. Khan, M. A. Khan, F. Qayyum, and D. H. Kim, “Evolving electric mobility energy efficiency: In-depth analysis of integrated electronic control unit development in electric vehicles,” *IEEE Access*, vol. 12, pp. 15957–15983, 2024.
- [6] M. U. Jan, A. Xin, H. U. Rehman, M. A. Abdelbaky, S. Iqbal, and M. Aurangzeb, “Frequency regulation of an isolated microgrid with electric vehicles and energy storage system integration using adaptive and model predictive controllers,” *IEEE Access*, vol. 9, pp. 14958–14970, 2021.
- [7] J. S. Kumar and N. S. Kumar, “Investigation of trajectory tracking fractional order controller for robot manipulator employing HIL simulation technique,” *Journal of Electrical Engineering*, vol. 16, no. 4, pp. 1–12, 2016.
- [8] A. Ibrahim, M. Salem, M. Swadi, and D. Ishak, “Power loss reduction of three-phase inverter in electric vehicle using variable switching frequency hybrid PWM,” *e-Prime-Advances in Electrical Engineering, Electronics and Energy*, vol. 10, p. 100876, 2024.
- [9] Z. Wang, J. Zhou, and G. Rizzoni, “A review of architectures and control strategies of dual-motor coupling powertrain systems for battery electric vehicles,” *Renewable and Sustainable Energy Reviews*, vol. 162, p. 112455, 2022.
- [10] W. Wu, J. H. Joloudari, S. K. Jagatheesaperumal, K. N. Rajesh, S. Gaftandzhieva, S. Hussain, R. Rabih, N. Haqjoo, M. Nazar, and H. Vahdat-Nejad, “Deep transfer learning techniques in intrusion detection system-internet of vehicles: A state-of-the-art review,” *Computers, Materials & Continua*, vol. 80, no. 2, 2024.
- [11] J. Liang, J. Feng, Z. Fang, Y. Lu, G. Yin, X. Mao, J. Wu, and F. Wang, “An energy-oriented torque-vector control framework for distributed drive electric vehicles,” *IEEE Transactions on Transportation Electrification*, vol. 9, no. 3, pp. 4014–4031, 2023.
- [12] A. Chantoufi, A. Derouich, N. E. Ouanjli, S. Mahfoud, A. E. Idrissi, A. F. Tazay, and M. I. Mosaad, “Direct torque control-based backstepping speed controller of doubly fed induction motors in electric vehicles: Experimental validation,” *IEEE Access*, 2024.
- [13] Y. Zhang, Y. Huang, Z. Chen, G. Li, and Y. Liu, “An optimal control strategy for plug-in hybrid electric vehicles based on enhanced model predictive control with efficient numerical method,” *IEEE Transactions on Transportation Electrification*, vol. 8, no. 2, pp. 2516–2530, 2022.

Biographies



Yang Yang received her master's degree from Liaoning University in 2012. Since 2015, she has been working at Liaoning University of Science and Technology, where her main research area is theoretical physics.

- [14] K. Li, F. Xiao, J. Liu, Z. Mai, C. Lian, S. Gao, and K. Fu, "Space vector pulsewidth modulation strategy for ANPC-5L inverter based on model predictive control," *IEEE Journal of Emerging and Selected Topics in Power Electronics*, vol. 11, no. 3, pp. 3020–3035, 2023.
- [15] H. Qi, M. Liwang, S. Hosseinalipour, L. Fu, S. Zou, and W. Ni, "Future resource bank for ISAC: Achieving fast and stable win-win matching for both individuals and coalitions," *arXiv preprint arXiv:2502.08118*, 2025.
- [16] A. Kazemtarghi, S. Dey, A. Mallik, and N. G. Johnson, "Asymmetric half-frequency modulation in DAB to optimize the conduction and switching losses in EV charging applications," *IEEE Transactions on Transportation Electrification*, vol. 9, no. 3, pp. 4196–4210, 2023.
- [17] S. Hou, H. Yin, B. Pla, J. Gao, and H. Chen, "Real-time energy management strategy of a fuel cell electric vehicle with global optimal learning," *IEEE Transactions on Transportation Electrification*, vol. 9, no. 4, pp. 5085–5097, 2023.
- [18] G. Priyanka, J. S. Kumar, and S. T. Veena, "Deep learning based video surveillance for predicting vehicle density in real time scenario," *Journal of Ambient Intelligence and Humanized Computing*, vol. 14, no. 4, pp. 4371–4383, 2023.
- [19] S. Chavan, B. Venkateswarlu, R. Prabakaran, M. Salman, S. W. Joo, G. S. Choi, and S. C. Kim, "Thermal runaway and mitigation strategies for electric vehicle lithium-ion batteries using battery cooling approach: A review," *Journal of Energy Storage*, vol. 72, p. 108569, 2023.
- [20] L. Tang, H. Xie, Y. Wang, and Z. Xu, "Deeply flexible commercial building HVAC system control: A physics-aware deep learning-embedded MPC approach," *Applied Energy*, vol. 388, p. 125631, 2025.
- [21] A. Rajamallaiah, S. P. K. Karri, M. L. Alghaythi, and M. S. Alshammari, "Deep reinforcement learning based control of a grid connected inverter with LCL-filter for renewable solar applications," *IEEE Access*, vol. 12, pp. 22278–22295, 2024.
- [22] E. Kontodinas, A. Kraemer, P. Karamanakos, and S. Wendel, "Optimal Modulation for Enhanced Performance of Electric Vehicle Drive Trains," *IEEE Journal of Emerging and Selected Topics in Power Electronics*, 2024.
- [23] M. Dong, M. Li, J. Zhou, Z. Wu, and L. Li, "3D sensing intermediate coils for receiver position identification and power enhancement in WPT system," *IEEE Transactions on Power Electronics*, 2025.
- [24] Q. Huang, Q. Huang, H. Guo, and J. Cao, "Design and research of permanent magnet synchronous motor controller for electric vehicle," *Energy Science & Engineering*, vol. 11, no. 1, pp. 112–126, 2023.
- [25] D. Zellouma, Y. Bekakra, and H. Benbouhenni, "Field-oriented control based on parallel proportional–integral controllers of induction motor drive," *Energy Reports*, vol. 9, pp. 4846–4860, 2023.
- [26] H. Qamar, H. Qamar, and R. Ayyanar, "Performance analysis and experimental validation of 240°-clamped space vector PWM to minimize common mode voltage and leakage current in EV/HEV traction drives," *IEEE Transactions on Transportation Electrification*, vol. 8, no. 1, pp. 196–208, 2021.
- [27] M. A. George, D. V. Kamat, and C. P. Kurian, "Electronically tunable ACO based fuzzy FOPID controller for effective speed control of electric vehicle," *IEEE Access*, vol. 9, pp. 73392–73412, 2021.
- [28] H. Chojaa, A. Derouich, O. Zamzoum, A. Watil, M. Taoussi, A. Y. Abdelaziz, Z. M. S. Elbarbary, and M. A. Mossa, "Robust control of DFIG-based WECS integrating an energy storage system with intelligent MPPT under a real wind profile," *IEEE Access*, vol. 11, pp. 90065–90083, 2023.